Influence of Terrestrial Cosmic Rays on the Reliability of CCD Image Sensors—Part 1: Experiments at Room Temperature

Albert J. P. Theuwissen, *Fellow, IEEE*

***Abstract*—An aging effect in solid-state image sensors is studied: the generation of hard errors resulting in hot spots, warm pixels, or white pixels. These effects even occur in image sensors that are simply stored on the shelf. This paper describes experiments that are set up to prove that the main origin can be found with neutrons that create displacement damage in the silicon bulk. These neutrons are part of terrestrial cosmic rays. This statement is based on measurements done on devices that we stored on the shelf, that were flown around the world in airplanes, that were stored at high altitude, and that were stored in an underground laboratory. The creation of the hot spots is independent of technology, architecture, sensor type, or sensor vendor, and it is observed in charge-coupled devices as well as in complementary metal–oxide–semiconductor image sensors. In other words, it is a typical issue of the semiconductor base material: silicon! The paper is split up into two parts: this paper (part 1) describes the experiments done at room temperature, part 2 will concentrate on experiments done at higher temperatures.**

***Index Terms*—CCD image sensors, CMOS image sensors, displacement damage, hot spots, radiation damage, terrestrial cosmic rays.**

I. Introduction

IT IS QUITE well known in the imaging community that image sensors are subject to degradation effects due to radiation. These effects show up as an increase in dark current, a loss in transfer efficiency [in the case of charge-coupled devices (CCDs)], and in the generation of extra "hot spots" [1], [2]. Devices intended for space applications are being fabricated in special processes so that the sensors can better withstand radiation and to make them radiation-hard. Question is whether similar effects are also responsible for the creation of hot pixels during normal on-the-self storage of image sensors. Simply storing imaging devices on the shelf does indeed result in a few extra "hot spots" over time. The problem is illustrated in Fig. 1, where a dark image generated by a particular imager at two time points separated by 1.5 years is shown. Notice the creation of a few extra hot spots (the horizontal line shape of the hot spots is due to the stretching of the image).

It is important to point out that these hot spots are permanent. It is not a soft error, in the sense that a high-energy particle was absorbed in the silicon, generated a cloud of charge carriers, and after the next image, all effects are gone. The effects investigated in this paper are hard errors: once they are created, they remain present in the imagers. This paper is the very first publication that will describe the origin of these hard errors, namely, terrestrial cosmic rays.

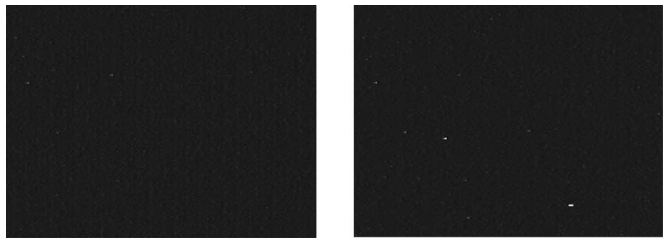

Fig. 1. Problem definition: two dark images (200 × 150 pixels out of a large image) taken by the same image sensor, time elapsed between the two pictures is 1.5 years.

II. Evaluation Method

To study the hot spot generation in the image sensors, an extensive measurement program is being developed. In its simplest form, devices were stored "on the shelf" and were measured at time intervals of several weeks. By comparing dark images obtained during various measurement cycles, research can be done to study the growth of hot spots. All measurements reported are done at 60 °C on CCD frame-transfer imagers with the following characteristics:

- active area of 8.8 (H) × 6.6 (V) mm^2;
- pixel size of 9 (H) × 22 (V) μm^2;
- collection depth of 2.5 μm;
- exposure time 20 ms;
- pixelclock 18 MHz.

The dark images were captured by a camera (internal gain setting: 256×, internal black level: 0), a 12-bit analog-to-digital converter (ADC), a frame-grabber, and a personal computer. The images were analyzed using conventional software tools.

Fig. 2 shows the basic measurement method: all amplitudes of all individual pixels of measurement n (in digital numbers (DN), with 1 DN = 2 pA/cm^2) are used as the X-coordinate, whereas the amplitudes of all individual pixels of measurement $n+1$ are used as the Y-coordinate. In this way, every pixel is represented by its two amplitudes (measurement n and measurement $n+1$) in a 2-D diagram. Ideally, all pixels are located on the straight line with slope = 1. In reality, and even

Manuscript received May 24, 2007. The review of this paper was arranged by Editor J. Tower.

The author is with Harvest Imaging, Kleine Schoolstraat, 9, 3960 Bree, Belgium (e-mail : albert@harvestimaging.com).

Color versions of one or more of the figures in this paper are available online at http://ieeexplore.ieee.org.

Digital Object Identifier 10.1109/TED.2007.908906

0018-9383/$25.00 © 2007 IEEE

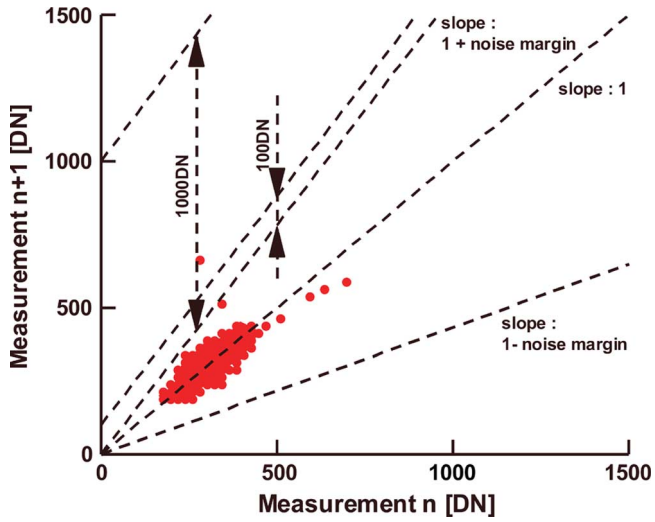

Fig. 2. Basic measurement method is illustrated. In an XY diagram, the creation of hot spots can be easily and clearly visualized.

in the case that the pixels do not change their value between the two measurements, there is always noise added to the pixel measurements. This noise is due to dark current shot noise and thermal noise of the sensor's output amplifier and of the camera electronics. Taking these noise sources into consideration in Fig. 2, the representation of all pixels is showing up as a cloud of measurement points with a mean value located on the line with slope $= 1$.

A pixel is defined as an extra hot spot if its $n+1$ measurement results in an amplitude larger than measurement n increased with a noise margin. The value of this noise margin is based on the dark current shot noise of measurement n, which is the read noise of the sensor. (The camera noise and the quantization noise of the ADC are negligible in comparison with the margin defined as such, even for small pixel amplitudes.)

The effect of this definition is also shown in Fig. 2 by means of the wedge around the curve with slope $= 1$. A pixel will be "earmarked" as being an extra hot spot when its representation on the XY diagram is located above the curve with slope $= 1$ plus the noise margin, or if

$$\text{meas}_{n+1} > \text{meas}_n + \text{noise}$$

where meas_{n+1} and meas_n represent the amplitudes of a certain pixel obtained in measurement $n+1$ and in measurement n, and noise represents the noise margin under consideration.

Once a pixel is recognized as a hot spot, its amplitude over which the pixel is grown between the two measurements is calculated, or

$$\text{growth\_amplitude} = \text{meas}_{n+1} - \text{meas}_n - \text{noise}.$$

Analysis of the data obtained is done by means of sequential measurements, of which the exact definition is shown in Fig. 3.

III. "On-the-Shelf" Storage at Sea Level

Devices were stored for a very long period on the shelf in Bree (N51°08′29″, E05°35′19″, 40 m above sea level, # device under test (DUT) $= 60$) and were measured at regular

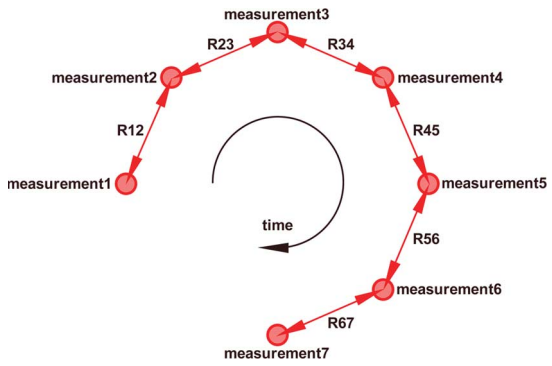

Fig. 3. Data analysis by means of sequential measurements.

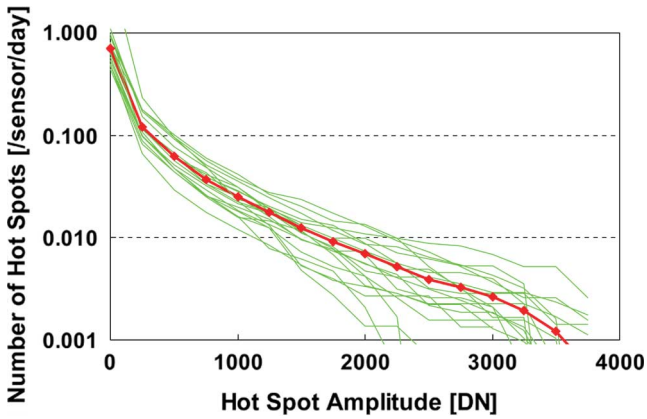

Fig. 4. Reverse cumulative probability of hot spot creation: the number of hot spots created per sensor and per day as a function of the amplitude of the hot spots (1 DN $= 2$ pA/cm^2). Every thin line represents the results of two measurement cycles; the thick line (with diamond symbols) represents the average of all measurements.

time intervals. Fig. 4 shows a typical result obtained from such a series of sequential measurements. On the horizontal axis, the amplitude of a newly grown hot spots (as defined in Section II) is shown, whereas the vertical axis shows the probability (per sensor and per day) that such a hot spot will be created. The data are represented in a reverse-cumulative histogram. Every thin line represents the result of two measurement cycles obtained from 60 sensors. These devices were stored on the shelf for periods of at least six weeks between two measurements. The thick solid line with diamond symbols shows the average behavior over a time period of almost five years.

From these results, it is clear that the generation of new hot spots can be relatively high, but it strongly depends on the amplitude of the hot spot. Notice the repeatability of the effects during this long testing period.

IV. Overseas Shipping of Devices

What can be the origin of these extra generated hot spots? Extensive tests were done to exclude the effect of cover glass, ceramic package, storage foam, shipping box, etc. Although it is known that all these materials can have an effect on the generation of soft errors, they had no effect at all on the creation of hard errors [3]. Shielding the imagers with lead (3 mm thickness) did not help either.

After an extensive literature search and discussions with many experts in the field, it is believed that the effect illustrated in Figs. 1 and 4 is due to high-energy cosmic rays, which are present even at sea level. Terrestrial cosmic rays are the results of very-high-energy particles created in space and/or by the sun, which hit the Earth's atmosphere [4]. These gigaelectronvolt particles create an avalanche effect on their way to the Earth surface. It is known that the energy and the density of cosmic rays is very dependent on altitude and latitude. In addition, the Earth's magnetic field plays an important role in directing the charged particles on their way. For this reason, the density of the cosmic rays is denser at the Earth's magnetic North Pole.

To prove the fact that terrestrial cosmic rays are the cause of the hot spot generation, and to check the dependency on altitude and latitude, sensors were shipped overseas by aircraft and by boat.

During all experiments, reference sensors were stored "on the shelf" and were used for comparison tests.

The results from a shipment by aircraft from Amsterdam (The Netherlands) to San Francisco (CA, USA) and Tokyo (Japan) are illustrated in Fig. 5(a) and (b). Both experiments were based on two trips back and forth. Every flight from Amsterdam to San Francisco or from Amsterdam to Tokyo, and vice versa takes about 12 h. Therefore, a complete trip back and forth corresponds to one day. In both figures, a reverse cumulative histogram shows (similar to Fig. 4) the increase in hot spot density. The reference curve is the one that is already shown in Fig. 4 as the average curve.

A few interesting remarks can be made.

- Notice the increase in probability to create extra hot spots. On the average, sending imagers back and forth from Amsterdam to San Francisco or to Tokyo corresponds to an increase in hot spots that is equivalent to a storage time of 100 days at sea level. This is fully in line with research done by IBM and Boeing. They found a failure rate of electronics at airplane altitudes to be about 100 times worse than at terrestrial altitudes [5], [6].
- Hot spots with a large amplitude seem to suffer more from this effect.
- The repeatability of the experiments is remarkable, the two trips in Fig. 5(a) or in Fig. 5(b) do not differ that much from each other, although there were several months in between the two trips.

It is known that the effect of cosmic rays is increasing with altitude and with latitude. Transporting imagers by aircraft from Amsterdam to San Francisco or to Tokyo brings the devices to a much higher altitude (33 000 ft) and to a higher latitude as well. Both parameters cannot be separated from each other in the experimental results, but their effect on the hot spot creation is obvious.

Image sensors were shipped from Rotterdam (The Netherlands) to Tokyo by boat as well: they left the harbor of Rotterdam for a trip of 40 days to Tokyo. Upon arrival, they were immediately returned by boat (another 40 days). After a total trip of 80 days, the sensors were analyzed again. The results are shown in Fig. 6.

If terrestrial cosmic rays are the origin of the hot spot generation, then shipping the sensors by boat must have a less-

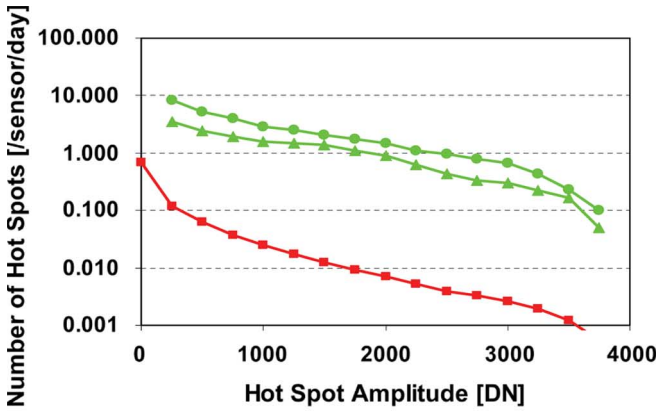

(a)

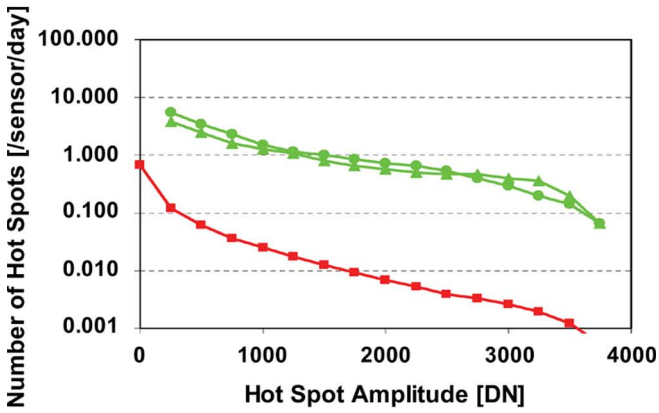

(b)

Fig. 5. (a) Results obtained after sending the imagers back and forth from Amsterdam to San Francisco by means of an airplane, two experiments are shown. The curves with the circle and triangle symbols represent the measurements, whereas the curve with the square symbols illustrates the reference material. (b) Results obtained after sending the imagers back and forth from Amsterdam to Tokyo by means of an airplane, two experiments are shown. The curves with the circle and triangle symbols represent the measurements, whereas the curve with the square symbols illustrates the reference material.

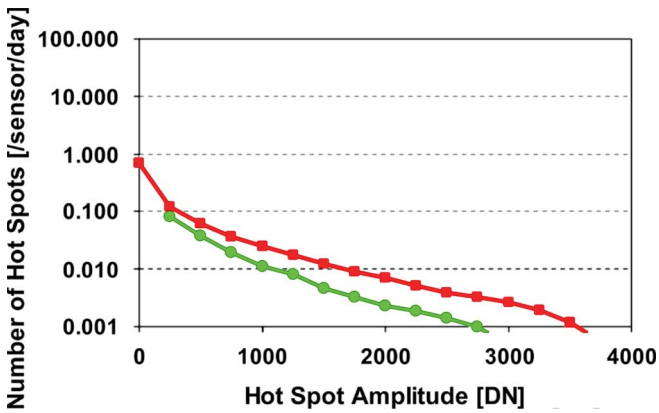

Fig. 6. Results obtained after sending the imagers back and forth from Rotterdam to Tokyo by boat. The curve with the circle symbols represents the measurements, whereas the curve with the square symbols illustrates the reference material.

pronounced effect than sending them by airplane. If the devices travel by boat, by definition, they stay at sea level. Fig. 6 proves this statement. Even a slight improvement can be seen. The explanation for this effect can be found in the route the boat

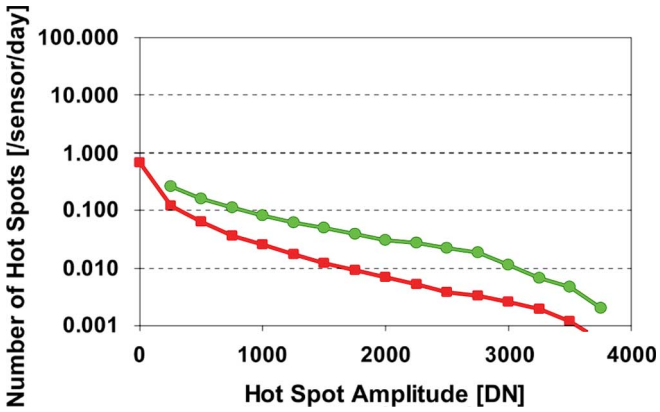

Fig. 7. Results obtained after storing the imagers for three months at Jungfraujoch (3450 m above sea level). The curve with the circle symbols represents the measurements, whereas the curve with the square symbols illustrates the reference material.

takes from Rotterdam to Tokyo. After leaving Rotterdam, the boat goes to the south, rounds South Africa, and continues then north to Tokyo. During this route, the boat moves away from the Earth's magnetic north pole, and actually, the sensors travel on a more favorable latitude [4].

V. "On-the-Shelf" Storage at Non-Sea Level

Another interesting experiment is the storage of the sensors at elevated altitude for a longer period of time. The devices were put on the shelf of a laboratory at Jungfraujoch (Switzerland, N46°32′51″, E7°58′56″, 3450 m above sea level, #DUT = 60) for a period of three months. After their return, they were immediately measured. The experimental results are shown in Fig. 7.

What could be expected came through, i.e., an increase in the number of hot spots. The ratio with the reference material is almost a factor of 10 for the large-amplitude hot spots, whereas for the small-amplitude hot spots, the ratio is closer to 5.

The second and last storage experiment was done underground, trying to completely shield the devices from cosmic rays. To totally protect the imagers from incoming cosmic rays, a concrete wall of 20 m is needed. The SCK Laboratory in Mol, Belgium (SCK is a study center for nuclear energy) is located at 250 m below sea level. Measurements performed by SCK employees proved that 250 m of clay ground is indeed more than enough to absorb all incoming cosmic rays. When the devices came back out the SCK laboratory (N51°12′51″, E5°5′9″, #DUT = 60), they were immediately analyzed, and the results are shown in Fig. 8.

The results of this experiment did not really confirm the following expectations.

- A factor of 10 to 1000 improvement could be seen for large-amplitude hot spots. Since the SCK Laboratory is absolutely free of cosmic rays, even more improvement was expected.
- Almost no improvement could be recognized for small-amplitude hot spots. This result is very surprising and indicates that probably more effects than just cosmic rays might influence the generation of hot spots. One possible explanation is the increase of dark current over time. A slight increase of the average value gives rise to the increase of dark fixed-pattern noise as well, and this can be seen as an increase in lower amplitude hot spots. Further investigation is needed to confirm this theory.

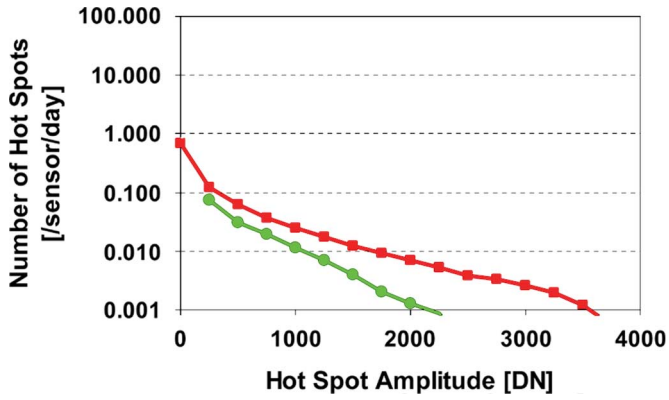

Fig. 8. Results obtained after storing the imagers for three months at SCK Laboratory (250 m below sea level). The curve with the circle symbols represents the measurements, whereas the curve with the square symbols illustrates the reference material.

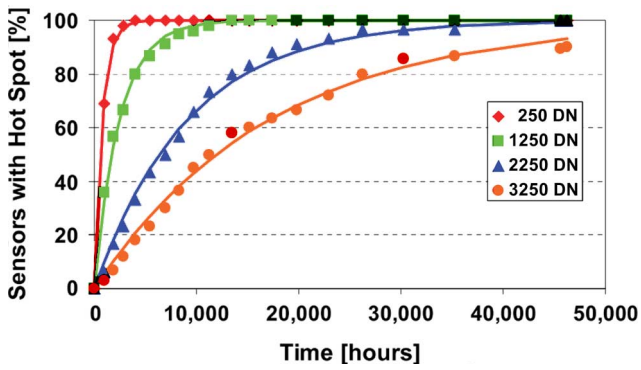

Fig. 9. Cumulative number of sensors showing an extra hot spot of 250 DN, 1250 DN, 2250 DN, and 3250 DN as a function of storage time. The dots represent the measured data, whereas the solid lines are exponentially fitted curves.

In conclusion for the SCK experiments, an improvement can be seen, but it is much less than expected. More research is needed to generate an explanation for this effect.

VI. Fitting the Experimental Data

Another way of presenting the results from the on-the-shelf-storage experiments is shown in Fig. 9. A cumulative histogram is shown, with the hours of storage on the horizontal axis and the cumulative number of sensors (percentage) that show an extra hot spot on the vertical axis. The dots shown in Fig. 9 are measurements obtained for hot spots with a value of 250 DN, 1250 DN, 2250 DN, and 3250 DN. The solid curves are fits through the measured points by means of an exponential curve, i.e.,

$$y = 100 \cdot (1 - e^{-a_x \cdot t})$$

in which t represents the storage time (in hours), and a_x is the fitting parameter (per hour) for hot spots of amplitude x DN.

For every hot spot amplitude, a fitted curve can be generated, and the fitting parameter a_x can be found. In this paper, hot

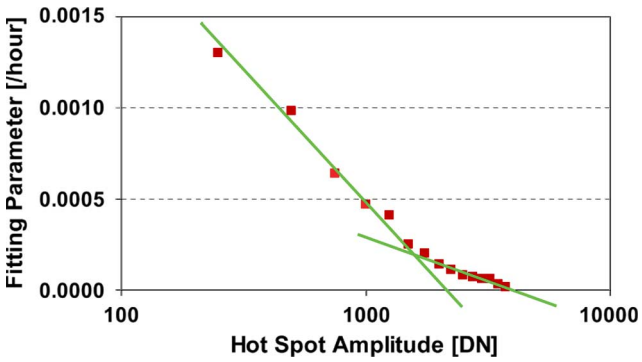

Fig. 10. Fitting parameter a_x as a function of the hot spot amplitude. The square dots represent the data obtained from the fitting, whereas the straight lines are trend lines that clearly mark two "types" of hot spots.

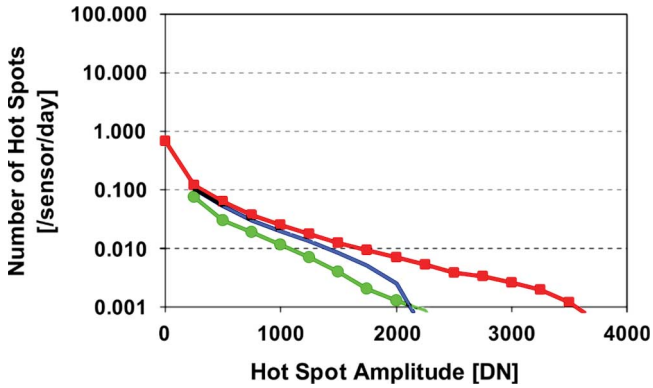

Fig. 11. Curve without symbols is calculated by subtracting the effects of the large-amplitude hot spots from the reference curve (solid line with the square symbols). The curve with the circle symbols is the measured one obtained from devices stored at −250 m.

spots with amplitude between 250 DN and 3750 DN with a step size of 250 DN are investigated. In Fig. 10, the exponent a_x, which is used as the fitting parameter in Fig. 9, is shown as a function of the amplitude of the hot spot. The squares are the results of the aforementioned curve-fitting exercise. The two straight lines are two fits to the empirically obtained data points.

It is noticeable that two groups of results can be recognized.

1) The data points for hot spots with larger amplitude correspond to relatively low values of the fitting exponent. These hot spots are most probably due to the damage of cosmic rays created in the bulk of the silicon. The energy of the cosmic rays is high enough to displace a silicon atom from its original location in the monocrystalline lattice. (Typically, a 150-keV electron can displace a silicon atom in the bulk lattice [7].) In this way, a vacancy as well as an interstitial are created. Vacancies created by incident radiation are unstable and migrate to energetically favorable positions in the lattice. Typically, the vacancies become trapped near impurity atoms due to the stress imposed on the lattice by the impurities. Typically, only 2% of the initially generated vacancies remain [8]. The line connecting the higher amplitude hot spot coefficients can be written as

$$a = 0.00222 - 0.00062 \cdot \log(\text{hot\_spot\_amplitude}).$$

2) The data points for hot spots with smaller amplitude correspond to relatively high values of the fitting exponent. These hot spots are most probably due to damage created at the Si–SiO_2 interface, due to the creation of extra surface states, and resulting as well in an overall increase of the dark current and dark-current fixed-pattern noise. (This statement is based on the fact that devices stored 250 m below sea level showed the same increase in dark current and dark-current fixed-pattern noise as devices stored at sea level.) The line connecting the lower amplitude hot spot coefficients is given by

$$a = 0.00575 - 0.00173 \cdot \log(\text{hot\_spot\_amplitude}).$$

Concentrating on the first equation, and in the assumption that the higher amplitude hot spots are created by cosmic rays, it is quite simple to calculate the number of hot spots generated per sensor and per day based only on that last equation. Subtracting this number of hot spots from the reference data, one obtains the result shown by the curve without symbols in Fig. 11: this corresponds to the theoretical hot spot generation without the effect of the cosmic rays. The curve with the circle symbols in Fig. 11 is the one obtained from storing the sensors at 250 m under the ground to shield them from terrestrial cosmic rays. The similarity between the two curves is surprising.

The coincidence of these two curves can be seen as a kind of proof that the large-amplitude hot spots are indeed created by the interaction of the silicon devices with terrestrial cosmic rays. Because at a depth of 250 m under the ground, no cosmic rays are present anymore. The effects of the terrestrial cosmic rays can be described by the equation given earlier (for this particular sensor under the specific measurement conditions).

VII. Nature of the Cosmic Rays

The cosmic rays that reach the Earth surface are so-called secondary rays. The primary cosmic rays come from the Milky Way and from the sun. These are mainly composed of protons with very high energies, ranging into the gigaelectronvolts. The primary cosmic rays collide with the various atoms and molecules of the atmosphere, and an avalanche effect is generating the secondary cosmic rays. These are composed of protons, pions, electrons, neutrons, muons, etc. The energy of the secondary cosmic rays is much lower than the energy of the primary ones but still can range into the megaelectronvolt [4].

The number of particles and the nature of the species composing the secondary cosmic rays can be calculated by some simple formulas. If I_1 is the cosmic ray flux at altitude A_1, and I_2 is the flux at altitude A_2 (both altitudes being expressed as an air pressure in grams per square centimeter), the relation between I_1 and I_2 is given by

$$I_2 = I_1 \cdot \exp\left(\frac{A_1 - A_2}{L}\right)$$

where L is a constant known as an absorption coefficient, depending on the nature of the cosmic rays (neutrons, protons, pions, muons, electrons, etc.).

To convert terrestrial altitudes to atmospheric pressure (in grams per square centimeter), the following relation can be

TABLE I
ABSORPTION COEFFICIENT OF THE VARIOUS COSMIC RAY SPECIES

	Absorption Coefficient (g/cm^2)
Electrons	100
Protons	110
Pions	110
Neutrons	148
Muons	520

TABLE II
ALTITUDES EXPRESSED IN GRAMS PER SQUARE CENTIMETER

	Atmospheric Pressure (g/cm^2)
Bree	1028
Jungfraujoch	701
Airplane trip	322

TABLE III
RATIO OF THE VARIOUS COSMIC RAY SPECIES BETWEEN JUNGFRAUJOCH AND BREE, AND AIRPLANE TRIPS AND BREE

	Jungfraujoch/Bree ratio	Airplane trip/Bree ratio
Electrons	26	1171
Protons	20	616
Pions	20	616
Neutrons	9	118
Muons	2	4

used:

$$A = 1033 - (0.03648 \cdot H) + (4.26 \cdot 10^{-7} \cdot H^2)$$

where H is the altitude in feet, and A is in grams per square centimeter (this assumes an average barometric pressure and a temperature of 0 °C).

The absorption coefficients for the various cosmic ray species are shown in Table I [4].

Taking into account the altitudes of Bree (40 m), Jungfraujoch (3450 m), and an airplane trip to Tokyo or San Francisco (10 000 m), it is possible to calculate the corresponding parameter A, which is expressed in grams per square centimeter. The results are shown in Table II.

With these data, it is relatively simple to calculate the ratio in electron, proton, pion, neutron, and muon concentration within the cosmic ray flux between Bree and Jungfraujoch on one hand, and between Bree and the airplane trips on the other hand. These results are shown in Table III.

Taking into account the data obtained from the airplane trips, as shown in Fig. 5(a) and (b), where an increase in number of hot spots is measured to be about a factor of 100, the conclusion might be made that the creation of hot spots is primarily due to neutrons. This statement is based on the fact that the density of neutrons in the cosmic ray flux is also a factor of about 100 higher during the airplane trips. The same conclusion can be drawn from the Jungfraujoch data: Fig. 8 shows an increase in hot spots by a factor of 10, almost exactly the same number is found for the increase in neutron density.

Comparing the measured data with the theoretical calculations, it might be concluded that neutrons from cosmic rays are the main source of the hot spot generation in solid-state imagers. On the other hand, the results obtained and the effects seen are fully in line with research data obtained from experiments with neutron radiation on image sensors [9].

VIII. CONCLUSION AND FUTURE WORK

The work presented in this paper can be summarized as follows.

— The number of white spots, hot points, or warm pixels in image sensors is increasing over time.
— This effect very strongly depends on the altitude at which the sensors are stored.
— This effect correlates very well with the number of neutrons present in the cosmic ray flux.

Based on the experiments described, the following conclusion can be made: the white spots, hot points, or warm pixels are due to cosmic rays, more specifically, the neutrons present in the cosmic ray flux cause displacement damage in the silicon bulk.

This statement implies that the creation of hot spots is independent of technology, architecture, sensor type, and sensor vendor. It is a typical issue of silicon. On the other hand, the exact amplitude of the hot spots can depend on pixel design and fabrication details. Therefore, the numbers listed in this paper will vary depending on the sensor type tested.

Based on all these conclusions, future work will concentrate on storage of the devices at elevated temperatures and how annealing affects the creation of cosmic ray damage. The results obtained in this paper will be published in part 2.

ACKNOWLEDGMENT

The author would like to thank L. Wilson, the late Prof. H. Debrunner, and the custodians of Jungfraujoch; M. Buyens of SCK Mol; A. Umans for his assistance in the hardware development; R. Langen for his assistance in the software development; G. Hopkinson (SIRA), D. Groom (LBNL Berkeley), and D. Denteneer (Philips Research) for their valuable discussions; and Philips Semiconductors/DALSA for supplying the sensors.

REFERENCES

[1] J. Janesick, *Scientific Charge-Coupled Devices*. Bellingham, WA: SPIE, 2001, pp. 722–725.
[2] G. Hopkinson *et al.*, "Proton effect in charge-coupled devices," *IEEE Trans. Nucl. Sci.*, vol. 43, no. 2, pp. 614–627, Apr. 1996.
[3] C. S. Dyer and P. R. Truscott, "Cosmic radiation effects on avionics," *Microprocess. Microsyst.*, vol. 22, no. 8, pp. 477–483, Feb. 1999.
[4] J. F. Ziegler, "Terrestrial cosmic rays," *IBM J. Res. Develop.*, vol. 40, no. 1, pp. 19–39, Jan. 1996.
[5] J. Olsen *et al.*, "Neutron-induced single event upsets in static RAMS observed at 10 km flight altitude," *IEEE Trans. Nucl. Sci.*, vol. 40, no. 2, pp. 74–77, Apr. 1993.
[6] A. Taber and E. Normand, "Single event upset in avionics," *IEEE Trans. Nucl. Sci.*, vol. 40, no. 2, pp. 120–126, Apr. 1993.
[7] J. Janesick *et al.*, "Radiation damage in scientific charge-coupled devices," *IEEE Trans. Nucl. Sci.*, vol. 36, no. 1, pp. 572–578, Feb. 1989.
[8] V. A. J. Van Lint, "The physics of radiation damage in particle detectors," *Nucl. Instrum. Methods Phys. Res. A, Accel. Spectrom. Detect. Assoc. Equip.*, vol. 253, no. 3, pp. 453–459, Jan. 1987.
[9] A. M. Chugg *et al.*, "Single particle dark current spikes induced in CCDs by high energy neutrons," *IEEE Trans. Nucl. Sci.*, vol. 50, no. 6, pp. 2011–2017, Dec. 2003.

Albert J. P. Theuwissen (S'80–M'80–SM'95–F'02) was born in Maaseik, Belgium, on December 20, 1954. He received the M.Sc. and Ph.D. degrees in electrical engineering from the Catholic University of Leuven, Leuven, Belgium, in 1977 and 1983, respectively. His thesis work was based on the development of supporting hardware around a linear CCD image sensor. His dissertation was on the implementation of transparent conductive layers as gate material in the CCD technology.

From 1977 to 1983, he was with the ESAT Laboratory, Catholic University of Leuven, where he focused on semiconductor technology for linear CCD image sensors. In 1983, he joined the Microcircuits Division, Philips Research Laboratories, Eindhoven, The Netherlands, as a Member of Scientific Staff. Since that time, he has been involved in the field of solid-state image sensing research, which resulted in the project leadership of SDTV and HDTV imagers. In 1991, he became the Department Head of the Division Imaging Devices, including CCD as well as CMOS solid-state imaging activities. He is the author or coauthor of many technical papers in the solid-state imaging field. In 1995, he authored a textbook *Solid-State Imaging with Charge-Coupled Devices*. He is the holder of several patents. In March 2001, he became a part-time Professor at the Delft University of Technology, Delft, The Netherlands, where he teaches courses in solid-state imaging and coaches Ph.D. students in their research on CMOS image sensors. From April 2002 till September 2007 he was with DALSA, originally as the CTO of the company and later as the Chief Scientist of DALSA Semiconductors. Since October 2007 he started his own company, Harvest Imaging, focusing on teaching, coaching and training in the field of solid-state imaging. He is also the Founder of the Walter Kosonocky Award, which highlights the best paper in the field of solid-state image sensors. He is a member of the editorial board of *Photonics Spectra* magazine.

In 1988, 1989, 1995, and 1996, he was a member of the International Electron Devices Meeting paper selection committee. He was a coeditor of the IEEE TRANSACTIONS ON ELECTRON DEVICES Special Issues on Solid-State Image Sensors, May 1991, October 1997, and January 2003, and of the IEEE Micro Special Issue on Digital Imaging, November/December 1998. In 1997 and 2003, he was the General Chairman of the IEEE International Workshop on Charge-Coupled Devices and Advanced Image Sensors, where he is also a member of the Steering Committee. For several years, he was a member of the Technical Committee of the European Solid-State Device Research Conference (ESSDERC) and the European Solid-State Circuits Conference (ESSCIRC). Since 1999, he has been a member of the Technical Committee of the International Solid-State Circuits Conference (ISSCC). He was a Secretary, a Vice-Chair, and a Chair in the European ISSCC Committee. He is a member of the overall ISSCC Executive Committee. He is nominated to be the Technical Program vice-chair and chair of ISSCC2009 and ISSCC2010 respectively. In 1998, he became an IEEE Distinguished Lecturer. He is a member of the SPIE.